# Optical Absorption Spectroscopy of the Tetranuclear Compound $[Mn\{Cu(oxpn)\}_3](ClO_4)_2 \cdot 2H_2O$ (oxpn = *N*,*N*′-Bis(3-aminopropyl)oxamide): Complementarity with Magnetic Properties

**Olivier Cador, Corine Mathonière,* and Olivier Kahn***

Laboratoire des Sciences Moléculaires, Institut de Chimie de la Matière Condensée de Bordeaux, CNRS UPR 9048, avenue du Docteur Schweitzer, 33608 Pessac, France

*Received July 18, 1996*[⊗]

The optical absorption spectroscopy of the tetranuclear compound $[Mn\{Cu(oxpn)\}_3](ClO_4)_2 \cdot 2H_2O$, with oxpn standing for *N*,*N*′-bis(3-aminopropyl)oxamide, has been investigated in the 4−300 K temperature range. The central $Mn^{II}$ ion is linked to three Cu(oxpn) complex ligands, so the molecular symmetry may be defined as $D_3$. The spectra, in addition to a d−d transition at 19 230 $cm^{-1}$ due to the $Cu^{II}$ ion in square planar surroundings, exhibit narrow and intense $Mn^{II}$ spin-forbidden transitions in the 24 300−28 750 $cm^{-1}$ range. These transitions are activated by an exchange mechanism. The temperature dependence of the main feature corresponding to the $^6A_1 \rightarrow {}^4A_1$, $^4E(G)$ $Mn^{II}$ transition was investigated. Using a model proposed first by Tanabe and co-workers and adapted to the $MnCu_3$ topology, a theoretical expression for the temperature dependence of the intensity of the transition has been established and compared with the experimental data. The only parameter of this expression is the interaction parameter $J$ between the local ground states ($\mathbf{H} = -J\sum_i \mathbf{S}_{Mn_i} \cdot \mathbf{S}_{Cu_i}$), which has been found to be −33.8 $cm^{-1}$. The energy of the transition has been found to be shifted by 47 $cm^{-1}$ toward the high energies as the temperature was lowered. A theoretical expression for the energy shift of the transition has been given. It depends on both $J$ and the interaction parameter $J^*$ between the $Cu^{II}$ ions in their ground states and the $Mn^{II}$ ion in the spin flip excited state. The comparison with the experimental data has led to a negative $J^*$ value of the same order of magnitude as the $J$ value. These results have been discussed in relation with the information deduced from magnetic measurements.

## Introduction

For several years we have been studying compounds containing $Mn^{II}Cu^{II}$ bimetallic species.[1−3] One of our main concerns was to synthesize molecular-based compounds exhibiting an ordered magnetic phase below the critical temperature $T_c$ in a controlled fashion. Along this line, we succeeded in designing and characterizing several types of molecular-based magnets, i.e., $Mn^{II}Cu^{II}$ ferrimagnetic chain compounds[4−7] and $Mn^{II}_2Cu^{II}_3$ ferrimagnetic two-dimensional networks.[8−10]

The field of molecular-based magnets has been increasingly attractive for 2 decades,[11] because these materials exhibit novel properties as compared to those of conventional permanent magnets. In particular, they have low density and usually are weakly colored. Promising opportunities could emerge for these materials in magneto-optical devices. However, until now, very few studies have been devoted to the optical properties of molecular-based magnets, in relation with their magnetic properties.[12−14] Of course, a great deal of effort has already concerned the spectroscopy of exchange-coupled systems, but essentially in doped compounds.[15]

Along this line, the $Mn^{II}Cu^{II}$ molecular compounds are interesting not only for their magnetic properties but also for their spectroscopic properties. Indeed, the absorption spectra show very intense bands associated with formally spin-forbidden $Mn^{II}$ transitions, activated by an exchange mechanism. The temperature dependence of both the intensity and the energy of these bands may provide quantitative information on the exchange mechanism. It is also possible to compare the results deduced from magnetic and optical measurements.

A few years ago, we investigated the optical properties of two $Mn^{II}Cu^{II}$ compounds, $[Mn(Me_6\text{-}[14]ane\text{-}N_4)Cu(oxpn)](CF_3SO_3)_2$, with $Me_6$-[14]ane-$N_4$ = (±)-5,7,7,12,14,14-hexamethyl-1,4,8,11-tetraazacyclotetradecane and oxpn = *N*,*N*′-bis(3-aminopropyl)oxamide,[16] and $\{[Mn(Me_6\text{-}[14]ane\text{-}N_4)]_2Cu(pba)\}(CF_3SO_3)_2 \cdot 2H_2O$, with pba = 1,3-propanediylbis(oxamato).[17] The structure of the former compound consists of binuclear units. The interaction between $S_{Mn} = {}^5/_2$ and $S_{Cu} = {}^1/_2$ local spins gives rise to two low-lying spin states, $S = 2$ and $S = 3$. In the excited states of $Mn^{II}$, the interaction between $S^*_{Mn} = {}^3/_2$ and $S_{Cu} = {}^1/_2$ gives rise to two spin states, $S^* = 2$ and $S^* = 1$. Selection rules applied on the spin of the pair result in a

[⊗] Abstract published in *Advance ACS Abstracts,* April 1, 1997.

(1) Pei, Y.; Verdaguer, M.; Kahn, O.; Sletten, J.; Renard, J.-P. *Inorg. Chem.* **1987**, *26*, 138.
(2) Kahn, O. *Struct. Bonding (Berlin)* **1987**, *68*, 89.
(3) Kahn, O. *Adv. Inorg. Chem.* **1995**, 43, 179.
(4) Kahn, O.; Pei, Y.; Verdaguer, M.; Renard, J.-P.; Sletten, J. *J. Am. Chem. Soc.* **1988**, *110*, 782.
(5) Nakatani, K.; Bergerat, P.; Codjovi, E.; Mathonière, C.; Pei, Y.; Kahn, O. *Inorg. Chem.* **1991**, *30*, 3977.
(6) Nakatani, K.; Carriat, J. Y.; Journaux, Y.; Kahn, O.; Lloret, F.; Renard, J.-P.; Pei, Y.; Sletten, J.; Verdaguer, M. *J. Am. Chem. Soc.* **1989**, *111*, 5739.
(7) Pei, Y.; Kahn, O.; Nakatani, K.; Codjovi, E.; Mathonière, C.; Sletten, J. *J. Am. Chem. Soc.* **1991**, *113*, 6558.
(8) Stumpf, H. O.; Ouahab, L.; Pei, Y.; Grandjean, D.; Kahn, O. *Science* **1993**, *261*, 447.
(9) Stumpf, H. O.; Ouahab, L.; Pei, Y.; Bergerat, P.; Kahn, O. *J. Am. Chem. Soc.* **1994**, *116*, 3866.
(10) Stumpf, H. O.; Pei, Y.; Kahn, O.; Sletten, J.; Renard, J.-P. *J. Am. Chem. Soc.* **1993**, *115*, 6738.
(11) Kahn, O. *Molecular Magnetism;* VCH: New York, 1993.
(12) Bellitto, C.; Day, P. *J. Chem. Soc., Dalton Trans.* **1978**, 1207.
(13) Bellitto, C.; Day, P.; Wood, T. E. *J. Chem. Soc., Dalton Trans.* **1986**, 847.
(14) Bellitto, C.; Day, P. *J. Mater. Chem.* **1992**, *2*, 265.
(15) Mac Carthy, P. J.; Güdel, H. U. *Coord. Chem. Rev.* **1988**, *88*, 69.
(16) Mathonière, C.; Kahn, O.; Daran, J.-C.; Hilbig, H.; Köhler, F. H. *Inorg. Chem.* **1993**, *32*, 4057.
(17) Mathonière, C.; Kahn, O. *Inorg. Chem.* **1994**, *33*, 2103.

S0020-1669(96)00857-9 CCC: $14.00 

unique transition $S = 2 \rightarrow S^* = 2$. The intensity of this transition varies with the thermal population of the $S = 2$ ground state, so the study of the temperature dependence of its intensity directly provides the value of the interaction parameter $J$. In that case, the agreement between the $J$ values deduced from magnetic measurements and spectroscopic data, respectively, was excellent. The structure of the latter compound consists of linear trinuclear units, with two $Mn^{II}$ ions at the extremities and the $Cu^{II}$ ion in the middle. The spin $S_{Cu} = {}^1/_2$ of $Cu^{II}$ interacts with the two spins $S_{Mn} = {}^5/_2$ of $Mn^{II}$. The energy levels scheme is more complex than that for the binuclear system. Nevertheless, selection rules based on symmetry considerations predict 16 transitions involving the $^4A_1(G)$ local state of $Mn^{II}$ (symmetry $O_h$). To follow the temperature dependence of the intensity, we introduced a formalism described first by Tanabe and coworkers.[18,19] This formalism accounts for the interaction between the incident light and a pair of coupled spins. Adapting this model to the trinuclear unit, we were able to determine the interaction parameter from the temperature dependence of the intensity of the band $^6A_1 \rightarrow {}^4A_1$, $^4E(G)$ of $Mn^{II}$ (symmetry $O_h$). The agreement with the magnetic data was again excellent. Moreover, information on the excited state was deduced from the shift of the maximum of the band versus temperature. All these results encouraged us to study other $Mn^{II}Cu^{II}$ systems of increasing complexity.

This paper is devoted to a new example of internal consistency between magnetic and optical properties for $Mn^{II}Cu^{II}$ compounds. It deals with a tetranuclear compound of formula $Mn[Cu(oxpn)]_3(ClO_4)_2$ (hereafter abbreviated as $MnCu_3$). The synthesis and the magnetic properties have been described elsewhere.[20] Using a Tanabe formalism adapted to the present molecular topology, the interaction parameters in both the ground and excited states will be determined. Moreover, a new feature will be reported: as the temperature is lowered, a new band appears which was not observed for the $Mn^{II}Cu^{II}$ compounds previously studied.

The molecular structure of $MnCu_3$ is not known accurately. By analogy with other $Mn^{II}Cu^{II}$ compounds whose structures were determined by X-ray diffraction[8−10] and with a $Cr^{III}Ni^{II}{}_3$ tetranuclear compound containing a similar bisbidentate bridge,[21] $MnCu_3$ may be represented as shown in Figure 1. The molecular symmetry may be idealized in $D_3$; the $Mn^{II}$ ion in an octahedral environment interacts with three $Cu^{II}$ ions in square planar environments of symmetry $D_{4h}$.

## Experimental Section

$MnCu_3$ was synthesized as described in ref 20, as a polycrystalline powder. The spectra were recorded with a CARY 5E spectrophotometer equipped with a continuous helium flow cryostat provided by Oxford Instruments. The lowest temperature we could reach was 3.8 K. At room temperature, $MnCu_3$ was investigated in acetonitrile solution. At low temperatures, it was investigated in thin cellulose acetate film, fixed in the cryostat with silver paint. These films were prepared as follows: 0.5 mmol of manganese(II) perchlorate dissolved in 10 mL of acetonitrile was added to a suspension of 1.5 mmol of Cu(oxpn) dissolved in 20 mL of acetonitrile. This mixture was added to a warm solution of cellulose acetate in acetonitrile. The resulting solution was poured in a Petri vase. Purple transparent films behaving as glasses were obtained 1 day after by evaporation of acetonitrile. We checked that these films contained only the title compound by comparison with a KBr pellet of the pure compound in the solid state: the optical spectra showed identical features and similar temperature dependences. The band intensities were calculated from the area delimited by the absorption band and a baseline common to all spectra. The shift in energy of the maximum of the band was determined with an accuracy of 5 $cm^{-1}$ in canceling the first derivative. The magnetic susceptibility of $MnCu_3$ was measured with a Quantum Design MPMS-5S SQUID magnetometer at 1000 G between 2 and 300 K.

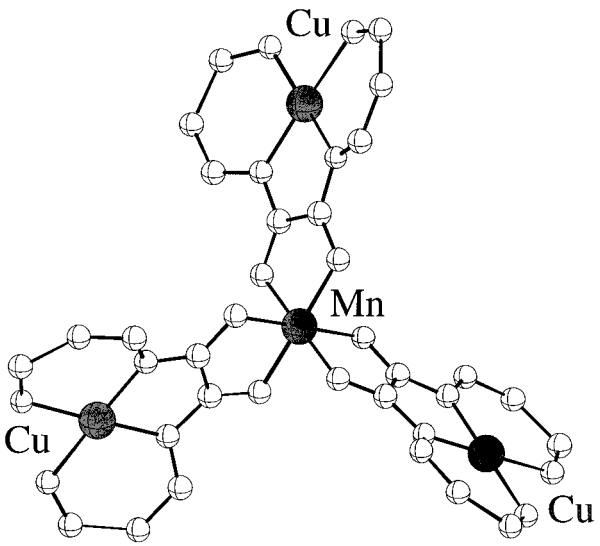


**Figure 1.** Schematic representation of the tetranuclear cation $[Mn\{Cu(oxpn)\}_3]^{2+}$.

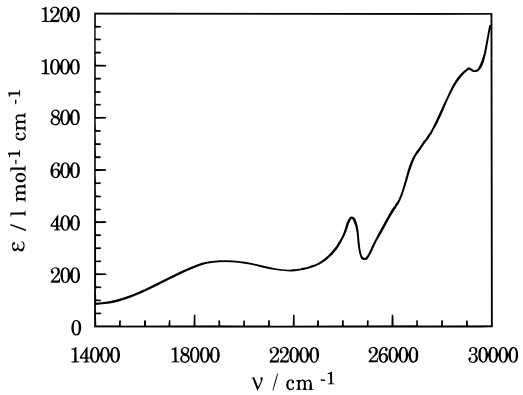


**Figure 2.** Absorption spectrum of $[Mn\{Cu(oxpn)\}_3](ClO_4)_2 \cdot 2H_2O$ in acetonitrile solution.

## Results

The magnetic properties were studied on a freshly prepared powder. The $\chi_M T$ versus $T$ curve, $\chi_M$ being the molar magnetic susceptibility and $T$ the temperature, follows the theoretical law given in ref 20. The parameters were estimated as $J = -27.5$ $cm^{-1}$, $g_{Mn} = 2.00$, and $g_{Cu} = 2.00$, where $J$ is the interaction parameter occurring in the Heisenberg Hamiltonian (formula 1) and $g_{Mn}$ and $g_{Cu}$ are the Zeeman factors associated with the $Mn^{II}$ and $Cu^{II}$ ions, respectively.

The solution spectrum of $MnCu_3$ at room temperature is shown in Figure 2. It exhibits a very broad band centered at 19 230 $cm^{-1}$ ($\epsilon = 256$ L $mol^{-1}$ $cm^{-1}$). Narrow bands appear in the higher energy range: 24 310 $cm^{-1}$ ($\epsilon = 511$ L $mol^{-1}$ $cm^{-1}$), 28 736 $cm^{-1}$ ($\epsilon = 1319$ L $mol^{-1}$ $cm^{-1}$), and a manifold between 26 000 and 27 000 $cm^{-1}$. The broad band at 19 230 $cm^{-1}$ corresponds to the $^2B_{1g} \rightarrow {}^2E_g$ transition of the $Cu^{II}$ ion in $D_{4h}$ local symmetry. The narrower band at 24 310 $cm^{-1}$ corresponds to the $^6A_{1g} \rightarrow {}^4A_{1g}$, $^4E_g(G)$ transition of the $Mn^{II}$ ion in $O_h$ local symmetry. This transition corresponds to a pure spin flip of an electron on the orbitals $t_{2g}$ or $e_g$ and is not influenced by the ligand field at the first order. The band at

(18) Ferguson, J.; Guggenheim, H. J.; Tanabe, Y. *J. Phys. Soc. Jpn.* **1966**, *21*, 692.
(19) Ferguson, J.; Guggenheim, H. J.; Tanabe, Y. *J. Chem. Phys.* **1966**, *45*, 1134.
(20) Lloret, F.; Journaux, Y.; Julve, M. *Inorg. Chem.* **1990**, *29*, 3967.
(21) Mitsumi, M.; Okawa, H.; Sakiyama, H.; Ohba, M.; Matsumoto, N.; Kurisaki, T.; Wakita, H. *J. Chem. Soc., Dalton Trans.* **1993**, 2291.

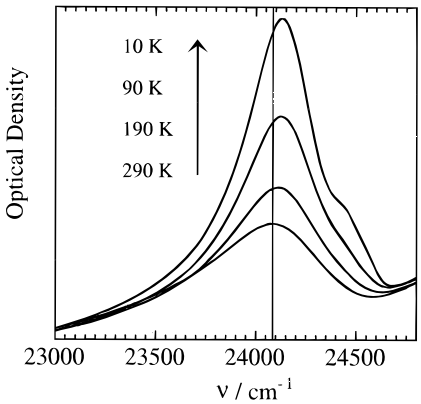


**Figure 3.** Absorption bands in the 22 500−25 000 $cm^{-1}$ range for [Mn{Cu(oxpn)}$_3$](ClO$_4$)$_2$·2H$_2$O in a cellulose acetate pellet at various temperatures.

28 736 $cm^{-1}$ can be assigned to the $^6A_{1g} \rightarrow {}^4E_g(D)$ transition and the manifold to the $^6A_{1g} \rightarrow {}^4T_{2g}(D)$ transition. The manifold may be explained by the splitting of the $^4T_{2g}(D)$ state under the effect of trigonal distortion and/or spin-orbit coupling.

The temperature studies of a thin acetate film in the range 4−300 K revealed no significant change for the $Cu^{II}$ transition. In contrast, a very pronounced enhancement of the intensity of $^6A_{1g} \rightarrow {}^4A_{1g}$, $^4E_g(G)$ was observed (see Figure 3). Moreover, the energy of the band was shifted from 24 080 $cm^{-1}$ at 300 K to 24 127 $cm^{-1}$ at 10 K, and a new band appeared below 130 K, centered approximatively at 24 460 $cm^{-1}$. The origin of this band will be discussed below. Using techniques described in the previous section, we are able to follow the temperature variation of the intensity of those bands as well as their position.

**Quantitative Interpretation**

We focused on the $^6A_{1g} \rightarrow {}^4A_{1g}$, $^4E_g(G)$ transition, which is the narrowest band in the spectra. All the previous works dealing with $Mn^{II}$ pairs have shown that the $^6A_{1g} \rightarrow {}^4A_{1g}$ is much more intense than the $^6A_{1g} \rightarrow {}^4E_g$.[22] In the following, we will assume that all the intensity comes from the $^6A_{1g} \rightarrow {}^4A_{1g}$ transition.

The spin Hamiltonian describing the interaction between the spins of the metal ions may be written as

$$\mathbf{H} = -J\mathbf{S}_{Mn}\cdot\mathbf{S}_{Cu} \tag{1}$$

$$\mathbf{S}_{Cu} = \mathbf{S}_{Cu3} + \mathbf{S}_{12}, \quad \mathbf{S}_{12} = \mathbf{S}_{Cu1} + \mathbf{S}_{Cu2} \tag{2}$$

where $J$ is the interaction parameter, and $\mathbf{S}_{Mn}$, $\mathbf{S}_{Cu1}$, $\mathbf{S}_{Cu2}$, and $\mathbf{S}_{Cu3}$ are the local spins. In (1), all the anisotropic factors as well as the possible interaction between the $Cu^{II}$ ions are neglected. This Hamiltonian leads to eight low-lying levels $|S,S_{Cu},S_{12}\rangle$ with the following energies:

$$E(S_{Mn},S_{Cu}) = -(J/2)[S(S+1) - S_{Cu}(S_{Cu}+1) - S_{Mn}(S_{Mn}+1)] \tag{3}$$

$S$, $S_{Mn}$, and $S_{Cu}$ are the quantum numbers associated with the spin operators $\boldsymbol{S} = \boldsymbol{S}_{Mn} + \boldsymbol{S}_{Cu}$, $\boldsymbol{S}_{Mn}$, and $\boldsymbol{S}_{Cu}$, respectively.

For the excited state corresponding to a spin flip on the $Mn^{II}$ ion, we define the spin operator $\boldsymbol{S}^*_{Mn}$. Moreover, we assume that the magnetic interaction in this excited state can be written in the same form as in the ground state. The validity of this assumption will be proved below. Therefore, we have

$$\mathbf{H}^* = -J^*\mathbf{S}^*_{Mn}\cdot\mathbf{S}_{Cu} \tag{4}$$

As in the ground state, this Hamiltonian leads to eight energy levels in this excited state. The ket basis may be written with the same quantum numbers as in the ground state, which leads to the same Lande splitting of the energy levels for the excited state (see Figure 5 below). It is interesting to note that some of the levels are degenerate, due to the fact that their energies do not depend on $S_{12}$. This happens in both the ground and excited states.

Let us now determine the symmetry labels of these levels. In $D_{4h}$ symmetry, the ground state of $Cu^{II}$ is $^2B_{1g}$. The coupling of the three $Cu^{II}$ ions in $D_3$ symmetry leads to two different labels. The states characterized by $S_{Cu} = {}^3/_2$ have $A_1$ symmetry, while the states characterized by $S_{Cu} = {}^1/_2$ have $E$ symmetry. Coupling further with $A_1$ of $Mn^{II}$ in $D_3$ symmetry gives rise to the $A_1$ and E molecule labels. The molecular states are written as $^3A_1$, $^5A_1$, $^5E$, $^7A_1$, $^7E$, $^9A_1$ in the ground state and $^1A_1$, $^3A_1$, $^3E$, $^5A_1$, $^5E$, $^7A_1$ in the excited state. The superscripts refer to the total spin degenerenacy of $MnCu_3$. Selection rules applied between ground and excited states give rise to eight subtransitions. No orbital restrictions occur; only spin restrictions do.

We are now faced with the calculation of the relative intensities of the eight subtransitions. As seen previously, the Hamiltonian describing the interaction between the incident light and the molecule is given by

$$\mathbf{H}_E = \sum_{i,j}(\prod_{Mn_iCu_j}\cdot\mathbf{E})(\mathbf{s}_{Mn_i}\cdot\mathbf{s}_{Cu_j}) \tag{5}$$

where $\mathbf{s}_{Mn_i}$ is a monoelectronic spin operator referring the $i$th 3d orbital of the $Mn^{II}$ ion, $\mathbf{s}_{Cu_j}$ is a spin operator referring to the singly occupied orbital on each $Cu^{II}$ ion, and $\mathbf{E}$ is the electric field of the incident light. The components of the vector $\prod_{Mn_iCu_j}$ are defined as

$$\prod^t_{Mn_iCu_j} = \left(\frac{\partial J_{i,j}}{\partial E^t}\right)_{E^t\rightarrow 0} \qquad t = x, y, z \tag{6}$$

$J_{i,j}$ is the interaction parameter between the $i$th 3d orbital of $Mn^{II}$ ion and the magnetic orbital of the $j$th $Cu^{II}$. The referential axes are represented in Figure 4.

Each element $Mn^{II}Cu^{II}_j$ has the $C_{2v}$ symmetry. In order for $\mathbf{H}_E$ to be totally symmetric, the vector $\prod_{Mn_iCu_j}$ and $\mathbf{E}$ must transform as the same irreducible representations of $C_{2v}$. It follows that the vectors $\prod_{Mn_iCu_j}$ are all parallel to the $C_2$ axis of the pairs $Mn^{II}Cu^{II}_j$. Therefore, using the axes defined in Figure 4, the $\prod_{Mn_iCu_j}$'s can be expressed as

$$\prod_{Mn_iCu_3} = \prod_{Mn_iCu_3}\mathbf{x}$$

$$\prod_{Mn_iCu_2} = -\frac{\sqrt{3}}{2}\prod_{Mn_iCu_2}\mathbf{y} - \frac{1}{2}\prod_{Mn_iCu_2}\mathbf{x} \tag{7}$$

$$\prod_{Mn_iCu_1} = \frac{\sqrt{3}}{2}\prod_{Mn_iCu_1}\mathbf{y} - \frac{1}{2}\prod_{Mn_iCu_1}\mathbf{x}$$

The symmetry of the molecule, together with the scheme coupling, gives the following relation between the $\prod_{Mn_iCu_j}$ components:

$$|\prod_{Mn_iCu_1}| = |\prod_{Mn_iCu_2}| = |\prod_{Mn_iCu_3}| \tag{8}$$

In the case of dipolar electric transitions, the transition moment vector $\mathbf{P}$ is defined as

(22) Ferguson, J.; Güdel, H. U.; Krausz, E. R.; Guggenheim, H. J. *Mol. Phys.* **1974**, *28*, 879.

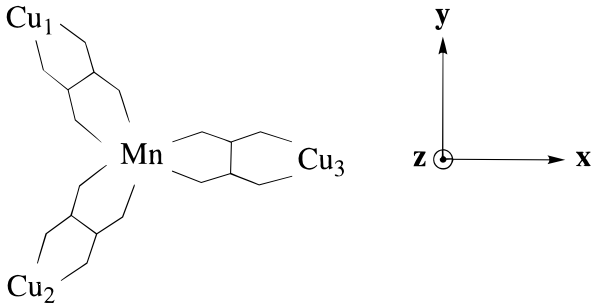


**Figure 4.** Reference axes adapted to the $MnCu_3$ topology.

$$\mathbf{P} = \sum_{i,j}\prod_{\mathrm{Mn}_i\mathrm{Cu}_j}(\mathbf{s}_{\mathrm{Mn}_i}\cdot\mathbf{s}_{\mathrm{Cu}_j}) \tag{9}$$

The subtransitions are all polarized in the *xy* plane (i.e., the plane containing the four metal ions). **P** acts only on the spin values. Then, the basis kets that have to be considered are in the form $|S,S_{\mathrm{Cu}},S_{12},S_{\mathrm{Mn}}\rangle$, in both the ground and excited states. The matrix element of the transition moment between states $|S,S_{\mathrm{Cu}},S_{12},S_{\mathrm{Mn}}\rangle$ and $|S',S'_{\mathrm{Cu}},S'_{12},S'_{\mathrm{Mn}}\rangle$ may be written as

$$\langle S,S_{\mathrm{Cu}},S_{12},S_{\mathrm{Mn}}|\mathbf{P}|S',S'_{\mathrm{Cu}},S'_{12},S'_{\mathrm{Mn}}\rangle = \langle S,S_{\mathrm{Cu}},S_{12},S_{\mathrm{Mn}}|\sum_{i,j}\prod_{\mathrm{Mn}_i\mathrm{Cu}_j}(\mathbf{s}_{\mathrm{Mn}_i}\cdot\mathbf{s}_{\mathrm{Cu}_j})|S',S'_{\mathrm{Cu}},S'_{12},S'_{\mathrm{Mn}}\rangle \tag{10}$$

Calculations based on the irreductible tensor theory[23] and symmetry considerations written above lead to the following expression for the **P** matrix elements:

$$\begin{aligned}\mathbf{P}(S,S_{\mathrm{Cu}},S_{12},S_{\mathrm{Mn}};S',S'_{\mathrm{Cu}},S'_{12},S'_{\mathrm{Mn}}) = (-1)^{S+S_{\mathrm{Cu}}+S'_{\mathrm{Mn}}+3/2}\delta_{S,S'}\times\\ \sqrt{\frac{3}{2}}\begin{Bmatrix}S'_{\mathrm{Mn}} & S'_{\mathrm{Cu}} & S\\ S_{\mathrm{Cu}} & S_{\mathrm{Mn}} & 1\end{Bmatrix}\sqrt{(2S_{\mathrm{Cu}}+1)(2S'_{\mathrm{Cu}}+1)}\times\\ A\left[(-1)^{S_{12}+S_{\mathrm{Cu}}}\delta_{S_{12},S'_{12}}\begin{Bmatrix}S_{\mathrm{Cu}} & 1 & S'_{\mathrm{Cu}}\\ 1/2 & S_{12} & 1/2\end{Bmatrix}\mathbf{x}+\right.\\ (-1)^{S'_{\mathrm{Cu}}}\sqrt{(2S_{12}+1)(2S'_{12}+1)}\begin{Bmatrix}S_{\mathrm{Cu}} & 1 & S'_{\mathrm{Cu}}\\ S'_{12} & 1/2 & S_{12}\end{Bmatrix}\times\\ \begin{Bmatrix}S_{12} & 1 & S'_{12}\\ 1/2 & 1/2 & 1/2\end{Bmatrix}\left[-1/2(1+(-1)^{S_{12}+S'_{12}})\mathbf{x}+\right.\\ \left.\left.\frac{\sqrt{3}}{2}(-1+(-1)^{S_{12}+S'_{12}})\mathbf{y}\right]\right]\end{aligned} \tag{11}$$

$$A = \sum_{i=1}^{5}\prod_{\mathrm{Mn}_i\mathrm{Cu}_3}\langle S_{\mathrm{Mn}}||\mathbf{s}_{\mathrm{Mn}_i}||S'_{\mathrm{Mn}}\rangle \tag{12}$$

The expressions between brackets are the $6-j$ symbols. From eq 11, the following spin selection rules are deduced: $\Delta S = 0$, $\Delta M_S = 0$, $\Delta S_{\mathrm{Mn}} = 0,\pm1$, $\Delta S_{\mathrm{Cu}} = 0,\pm1$. The molecular symmetry leads to another selection rule: the transitions with $\Delta S_{\mathrm{Cu}} = 0$ and $S_{\mathrm{Cu}} = 3/2$ have zero intensity. Finally, we end up with five subtransitions. The energy levels of the ground and excited states, as well as the five subtransitions, are summarized in Figure 5. Each subtransition $|S,S_{\mathrm{Cu}},S_{12}\rangle \rightarrow |S',S'_{\mathrm{Cu}},S'_{12}\rangle$ has an intensity relative to the intensity of $|1,3/2,1\rangle \rightarrow |1,1/2,1\rangle + |1,1/2,0\rangle$, given by

$$I(S,S_{\mathrm{Cu}}) = \frac{\sum_{S',S'_{\mathrm{Cu}},S'_{12},S_{12}} P^2(S,S_{\mathrm{Cu}},S_{12},5/2;S',S'_{\mathrm{Cu}},S'_{12},3/2)}{\sum_{S'_{12}} P^2(1,3/2,1,5/2;1,1/2,S'_{12},3/2)} \tag{13}$$

(23) Weissbluth, M. *Atoms and molecules*; Academic Press: London, 1978.

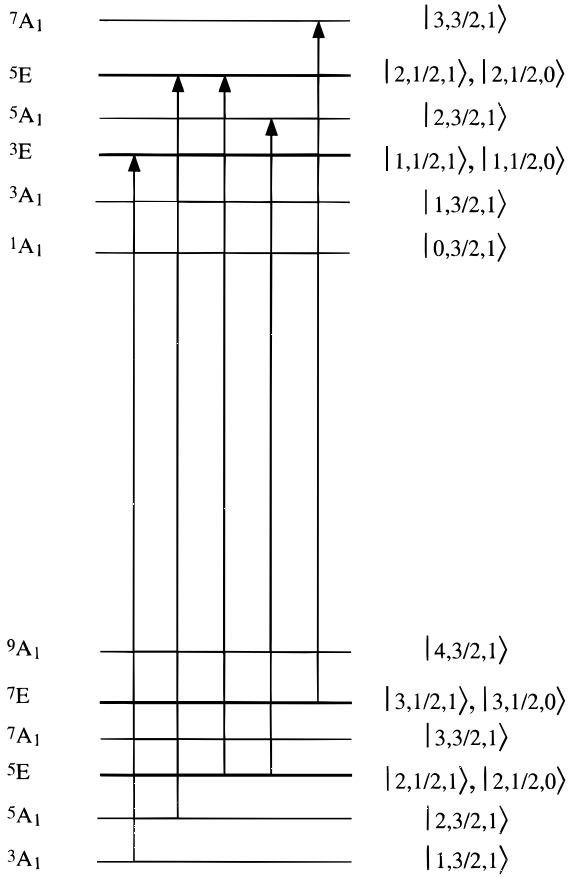


**Figure 5.** Relative energies and symmetry labels for the low-lying and excited states of $[Mn\{Cu(oxpn)\}_3](ClO_4)_2\cdot 2H_2O$ and optical subtransitions.

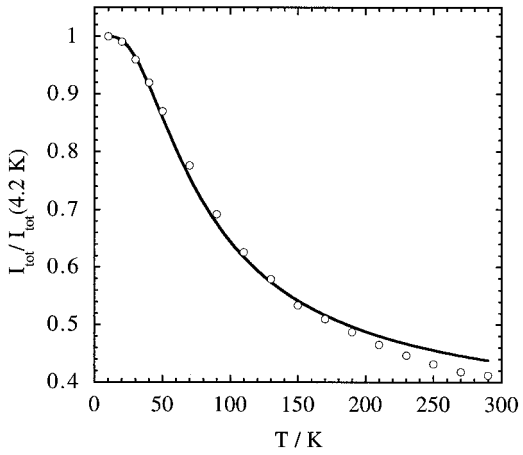


**Figure 6.** Temperature dependence of the absorption band at 24 080 $cm^{-1}$ for $[Mn\{Cu(oxpn)\}_3](ClO_4)_2\cdot 2H_2O$: (○) experimental data and (—) calculated curve.

Values of $I(S,S_{\mathrm{Cu}})$ and of the square of the transition moments are given in Table 1. The temperature dependence of the intensity, $I_{\mathrm{relat}}(T)$, is then calculated as

$$I_{\mathrm{relat}}(T) = \frac{\sum_{S,S_{\mathrm{Cu}}}(2S+1)I(S,S_{\mathrm{Cu}})\exp\left(-\frac{E(S,S_{\mathrm{Cu}})}{kT}\right)}{\sum_{S,S_{\mathrm{Cu}}}(2S+1)\exp\left(-\frac{E(S,S_{\mathrm{Cu}})}{kT}\right)} \tag{14}$$

where $I_{\mathrm{relat}}(0)$ is taken as unity. Least-squares fitting of the experimental data leads to $J = -33.8\ cm^{-1}$. Both theoretical and experimental curves are compared in Figure 6. Let us recall

**Table 1.** Transition Moments and Relative Intensities of Subtransitions

| subtransition | $P^2(S,S_{Cu},S_{12},{}^5/_2;S',S'_{Cu},S'_{12},{}^3/_2)$ | $I(S,S_{Cu})$ |
|---|---|---|
| $\|1,{}^3/_2,1\rangle \rightarrow \|1,{}^3/_2,1\rangle$ | 0 | |
| $\|1,{}^3/_2,1\rangle \rightarrow \|1,{}^1/_2,1\rangle$ | 0.5 | 1 |
| $\|1,{}^3/_2,1\rangle \rightarrow \|1,{}^1/_2,0\rangle$ | 0.5 | |
| $\|2,{}^3/_2,1\rangle \rightarrow \|2,{}^3/_2,1\rangle$ | 0 | |
| $\|2,{}^3/_2,1\rangle \rightarrow \|2,{}^1/_2,1\rangle$ | 0.233 | 0.467 |
| $\|2,{}^3/_2,1\rangle \rightarrow \|2,{}^1/_2,0\rangle$ | 0.233 | |
| $\|2,{}^1/_2,1\rangle \rightarrow \|2,{}^3/_2,1\rangle$ | 0.067 | |
| $\|2,{}^1/_2,1\rangle \rightarrow \|2,{}^1/_2,1\rangle$ | 0.267 | |
| $\|2,{}^1/_2,1\rangle \rightarrow \|2,{}^1/_2,0\rangle$ | 0.267 | 1.2 |
| $\|2,{}^1/_2,0\rangle \rightarrow \|2,{}^3/_2,1\rangle$ | 0.067 | |
| $\|2,{}^1/_2,0\rangle \rightarrow \|2,{}^1/_2,1\rangle$ | 0.267 | |
| $\|2,{}^1/_2,0\rangle \rightarrow \|2,{}^1/_2,0\rangle$ | 0.267 | |
| $\|3,{}^3/_2,1\rangle \rightarrow \|3,{}^3/_2,1\rangle$ | 0 | 0 |
| $\|3,{}^1/_2,1\rangle \rightarrow \|3,{}^3/_2,1\rangle$ | 0.333 | 0.333 |
| $\|3,{}^1/_2,0\rangle \rightarrow \|3,{}^3/_2,1\rangle$ | 0.333 | 0.333 |

**Table 2.** Relative Energies of Subtransitions

| subtransition | $E(S,S_{Cu};S',S'_{Cu})$ |
|---|---|
| $\|1,{}^3/_2\rangle \rightarrow \|1,{}^1/_2\rangle$ | 0 |
| $\|2,{}^3/_2\rangle \rightarrow \|2,{}^1/_2\rangle$ | $2J - 2J^*$ |
| $\|2,{}^1/_2\rangle \rightarrow \|2,{}^3/_2\rangle$ | $7J/2 - J^*/2$ |
| $\|2,{}^1/_2\rangle \rightarrow \|2,{}^1/_2\rangle$ | $7J/2 - 2J^*$ |
| $\|3,{}^1/_2\rangle \rightarrow \|3,{}^3/_2\rangle$ | $13J/2 - 7J^*/2$ |

that the interaction parameter deduced from magnetic data is $-27.5$ cm$^{-1}$.

Let us come back to the energy shift of the band in the range 4−300 K. To interpret this shift, the energy of the subtransitions must be examined very carefully. In Figure 5, $J^*$ was assumed to be negative. The energy of each subtransition depends on the two parameters $J$ and $J^*$. These energies are tabulated in Table 2. Assuming that the subtransitions have the same bandwidth and that this bandwidth is not changing in the studied temperature range, the subtransitions may be reproduced with Gaussian shapes. From Table 2 and the ground state Boltzmann populations, the profile of the local $^6A_1 \rightarrow {}^4A_1$ transition can be represented as a function of temperature. A theoretical spectrum can be built with the function $s(J, J^*,T,\upsilon,\omega)$, defined as

$$s(J,J^*,T,\upsilon,\omega) = \frac{\sum_{S,S_{Cu}} (2S+1)g(\upsilon,\omega;E(S,S_{Cu};S',S'_{Cu}))I(S,S_{Cu}) \exp\left(-\frac{E(S,S_{Cu})}{kT}\right)}{\sum_{S,S_{Cu}} (2S+1) \exp\left(-\frac{E(S,S_{Cu})}{kT}\right)} \quad (15)$$

where $g(\upsilon,\omega;E(S,S_{Cu};S',S'_{Cu}))$ is a Gaussian function written as

$$g(\upsilon,\omega;E(S,S_{Cu};S',S'_{Cu})) = \exp\left(-\left(\frac{2\sqrt{\ln 2}(\upsilon - E(S,S_{Cu};S',S'_{Cu}))}{\omega}\right)^2\right) \quad (16)$$

where $\upsilon$ is the energy of the incident photon, $\omega$ is the bandwidth, and $E(S,S_{Cu};S',S'_{Cu})$ is the transition energy given in Table 2. The position of the band is determined by canceling the first derivative of $s(J,J^*,T,\upsilon,\omega)$ with respect to $\upsilon$.The problem was solved numerically by fixing $J$, $J^*$, $\omega$, and $T$. The best results are obtained with $J^* = -45$ cm$^{-1}$ in the 4−170 K range. The simulations with $J = -33.8$ cm$^{-1}$, $\omega = 300$ cm$^{-1}$, and $J^* = -45$, 0, $+45$ cm$^{-1}$ are compared to the experimental data in Figure 7. The uncertainty on the $J^*$ value is probably rather large and difficult to estimate. However, the comparisons in Figure 7 emphasize that $J^*$ is negative. As a matter of fact, for a positive $J^*$ value the energy of the band would be much more temperature dependent. The discrepancies at higher temperature will be discussed below.

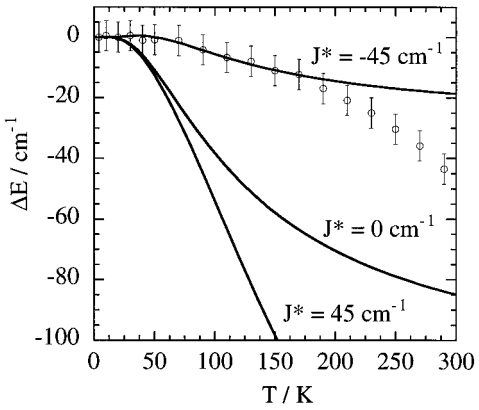


**Figure 7.** Energy shift of the absorption band $\Delta E = E_0(T) - E_0(4.2\ K)$ at 24 130 cm$^{-1}$ for $[Mn\{Cu(oxpn)\}_3](ClO_4)_2 \cdot 2H_2O$: (○) experimental data and (—) calculated curves (see text).

## Discussion and Conclusion

This paper is the third one dealing with the optical absorption properties of $Mn^{II}Cu^{II}$ compounds. Having started with the simplest pattern, a dinuclear unit MnCu, and then following with a trinuclear unit MnCuMn, we have been studying here a tetranuclear unit $MnCu_3$. All these compounds show several $Mn^{II}$ spin-forbidden transitions activated by an exchange mechanism. We focused on the $^6A_1 \rightarrow {}^4A_1$, $^4E(G)$ (symmetry $O_h$) transition corresponding to a spin flip of an electron in its orbital. As the nuclearity of the compounds increases, the Tanabe formalism used to interpret the temperature dependence of both the intensity and the energy shift of the band becomes more sophisticated. However, we can now draw some general conclusions concerning the optical properties of these systems. (i) The Tanabe formalism describes fairly well the temperature dependence of the intensity of the band. For $MnCu_3$, it gives rise to five subtransitions, all polarized in the plane containing the four metal ions. A $J$ value of $-33.8$ cm$^{-1}$ was determined. This value is slightly higher (in absolute value) than that deduced from magnetic susceptibility measurements ($-27.5$ cm$^{-1}$). A similar difference was observed for MnCuMn. These differences are probably due to the approximations inherent to the theory. Indeed, the model based on symmetry considerations is not valid anymore if the compound deviates from the ideal symmetry ($D_{2h}$ for MnCuMn and $D_3$ for $MnCu_3$). (ii) For all the $Mn^{II}Cu^{II}$ systems we studied, we noticed an asymmetry of the $^6A_1 \rightarrow {}^4A_1$, $^4E(G)$ (symmetry $O_h$) transition on the low-energy side of the band. Moreover, for $MnCu_3$, a new feature appears at higher energy as the temperature is lowered. This new feature is present in all the compounds studied so far with the $D_3$ symmetry around the $Mn^{II}$ ion.[24] In the theoretical treatment, we have neglected the contribution of the $^4E(G)$ state. In fact, the $^4A_1$ and $^4E(G)$ states are not degenerate when the symmetry is lower than $O_h$. In $D_3$ symmetry, normalized spherical harmonic (NSH) potential calculations have shown that the $^4E$ state is below the $^4A_1$ state, whatever the distortion of the octahedron (elongation or compression) may be.[25] It is clear that the low-energy asymmetry of the band is related to an intensity provided by the $^4E(G)$ state. This does not change

(24) Cador, O.; Mathonière, C.; Kahn, O. Unpublished results.
(25) Hempel, J. C. *J. Chem. Phys.* **1976**, *64*, 4307.

the intensity mechanism developed above. Indeed, taking into account the $^4E$ state changes only the **Π** coefficient values. The relative intensities of the transitions were determined, irrespective of these values, so that the model remains valid if we consider both the $^4A_1$ and $^4E$ states. To sum up, in all our compounds the low-energy side of the 24 100−24 500 $cm^{-1}$ bands can partially be assigned to a $^4E$ state component. Then we are faced with the origin of the new feature at higher energies for $MnCu_3$. This cold band appears at 333 $cm^{-1}$ above the major one at 10 K. It is more strongly temperature dependent in the 5−100 K range than the main feature, raising up in a ratio 5:1. Further studies will be necessary to specify the origin of this band. We can say that this band is associated with the $D_3$ topology. (iii) For the second time we have been able to estimate the interaction parameter in the first excited state. The energy shift of the band has been simulated by a theoretical law derived from the model developed above. When $J^*$ is fixed at $-45$ $cm^{-1}$, the experimental shifts are correctly reproduced in the 4−170 K range. At higher temperature, the discrepancy between experimental and theoretical curves increases with the temperature. Our model does not take account of the asymmetry of the band, which becomes more and more pronounced above 170 K. We suppose that this asymmetry influences the position of the absorption band maximum. This could explain the deviation of the experimental data with respect to the theoretical ones. Finally, we determined a negative value indicating an antiferromagnetic coupling in the excited state as in the ground state. That seems reasonable because the $J$ and $J^*$ values are governed by a strongly antiferromagnetic term involving two magnetic orbitals located in the same plane and pointing to each other.

The optical and magnetic techniques allowed us to investigate the ground states as well as the optically reached excited states. The magnetic techniques are a probe of the sublevels in the ground state, whereas the optical techniques imply only some levels of the ground and excited states. Nevertheless, the agreement between information deduced from both techniques is very satisfying.

To summarize, we have shown the consistency and the complementarity between the optical and magnetic techniques for paramagnetic $Mn^{II}Cu^{II}$ molecules. In the future, we would like to extend these studies to infinite $Mn^{II}Cu^{II}$ systems. In particular, we would like to study the effect of a long-range magnetic ordering on the optical properties.

## Safety Note

Perchlorate salts of metal complexes with organic ligands are potentially explosive. In the synthesis described here, we used only small amounts of material (the preparations were carried out at the millimole scale), and the starting perchlorate salt was an aquo complex. The dilute solutions were handled with great caution and evaporated slowly at room temperature.[26]

IC960857Q

(26) (a) *J. Chem. Educ.* **1973**, *50*, A335. (b) *Chem. Eng. News* **1983**, *61*, 4; **1963**, *41*, 47.